[American Journal of Science, Vol. 308, June, 2008, P. 770–786, DOI 10.2475/06.2008.02]

RESOLVING MILANKOVITCH: CONSIDERATION OF SIGNAL AND NOISE

STEPHEN R. MEYERS*,†, BRADLEY B. SAGEMAN**, and MARK PAGANI***

ABSTRACT. Milankovitch-climate theory provides a fundamental framework for the study of ancient climates. Although the identification and quantification of orbital rhythms are commonplace in paleoclimate research, criticisms have been advanced that dispute the importance of an astronomical climate driver. If these criticisms are valid, major revisions in our understanding of the climate system and past climates are required. Resolution of this issue is hindered by numerous factors that challenge accurate quantification of orbital cyclicity in paleoclimate archives. In this study, we delineate sources of noise that distort the primary orbital signal in proxy climate records, and utilize this template in tandem with advanced spectral methods to quantify Milankovitch-forced/paced climate variability in a temperature proxy record from the Vostok ice core (Vimeux and others, 2002). Our analysis indicates that Vostok temperature variance is almost equally apportioned between three components: the precession and obliquity periods (28%), a periodic "100,000" year cycle (41%), and the background continuum (31%). A range of analyses accounting for various frequency bands of interest, and potential bias introduced by the "saw-tooth" shape of the glacial/interglacial cycle, establish that precession and obliquity periods account for between 25 percent to 41 percent of the variance in the 1/10 kyr – 1/100 kyr band, and between 39 percent to 66 percent of the variance in the 1/10 kyr – 1/64 kyr band. These results are approximately two to four times greater than those published by Wunsch (2004) for the same Vostok time series. In all cases, most of the remaining variance is accounted for by the "100,000" year cycle, which is distinct from a background continuum that resembles autoregressive "red noise." Our analysis highlights the importance of a comprehensive assessment of the climate signals in geologic records, and underscores the significance of orbital forcing/pacing as a primary agent of Pleistocene climate change.

INTRODUCTION

Since the influential work of Hays and others (1976), identification and quantification of Milankovitch orbital periodicities in Cenozoic and Mesozoic proxy records have become a foundation for paleoclimate research. Paleoclimate records that preserve a response to orbital variations are now commonly employed to assess the controls on past climate change, and to constrain high-resolution chronologies for Pleistocene and deep-time research. Despite the proliferation of studies that identify and utilize the orbital signal preserved in proxy records, skepticism remains regarding the relative importance of changes in orbital-insolation on paleoclimate variability (for a review, see Elkibbi and Rial, 2001). For example, strong eccentricity band signals observed in many paleoclimate records (for example, Olsen, 1986; Herbert and Fischer, 1986; Sageman and others, 1997; Weedon and Jenkyns, 1999; Shackleton, 2000; Zachos and others, 2001) are difficult to justify because insolation changes on this timescale are relatively small compared to those of precession and obliquity. Other studies have suggested that stochastic processes could account for all or most of the observed variability in putative orbitally forced/paced paleoclimate records (for

*University of North Carolina at Chapel Hill, Department of Geological Sciences, Chapel Hill, North Carolina 27599, USA

**Northwestern University, Department of Geological Sciences, Evanston, Illinois 60201, USA

***Yale University, Department of Geology and Geophysics, P.O. Box 208109, New Haven, Connecticut 06520-8109, USA

†Corresponding author: smeyers@email.unc.edu

example, Kominz and Pisias, 1979; Saltzman, 1982; Pelletier, 2002; Wunsch, 2003, 2004). If changes in insolation, as a result of orbital variability, are not intrinsically tied to the pattern of past climate change observed in various geologic archives, major revisions in our understanding of the climate system are required.

From a practical point of view, resolution of this debate is hindered by difficulties associated with the accurate characterization of orbital signals preserved in paleoclimate archives. The intent of this study is to bring attention to the wide range of factors that must be carefully considered when quantifying orbital signals in paleoclimate proxy data, and to provide a new template for such analyses. Emphasis is placed on a comprehensive assessment of the noise introduced into the proxy record as the orbital-insolation signal propagates from primary climate response to the final data subjected to time series analysis.

We apply this approach to evaluate a proxy temperature record from the Vostok ice core (Vimeux and others, 2002), representing one of the most well-constrained time series of late Pleistocene climate change. Although climate signals preserved in the Vostok ice core have been previously interpreted as recording a strong orbital signal (for example, Shackleton, 2000), a recent analysis of this proxy temperature series suggests that orbital changes account for no more than 7 percent of its variability (Wunsch, 2004). If correct, the absence of a strong orbital signature in the Vostok record would cast doubt on the significance of orbital signals in more poorly constrained proxy data that are typical of most Pleistocene and deep-time paleoclimate studies. As will be shown, precession and obliquity signals in fact account for a substantial component of climate variability, and a strongly periodic 100,000 year cycle accounts for most of the remaining variance. In contrast to previous analyses of this record (Wunsch, 2004), we also demonstrate that broadband stochastic noise represents no more than 31 percent of the temperature variance (potentially much less). We also find that a simple autoregressive noise model is useful for describing the overall background structure of the data (in agreement with Wunsch, 2004).

Based on these observations, we argue that the Milankovitch-climate theory remains robust and that most criticisms of an orbit-climate linkage fail to recognize the inherent propagation and distortion (noise) of orbital signals captured in proxy records. If a comprehensive assessment of noise introduced into the proxy record is considered, orbitally forced/paced signals comprise the majority of climate variance in the Vostok temperature proxy.

THE PATHWAY OF THE ORBITAL SIGNAL

As the orbital-insolation signal propagates through the climate system and into various depositional systems, it is subject to distortion (including diminution or amplification) by a wide range of processes (for example, Goreau, 1980; Pestiaux and Berger, 1984; Ripepe and Fischer, 1991; Herbert, 1994; Clark and others, 1999; Meyers and others, 2001; Laurin and others, 2005). In addition, sampling of the preserved paleoclimate record, and the construction of proxy climate variables from the paleoclimate archive, can further distort the observed orbital signal. To address these concerns, figure 1 outlines the general pathway of the orbital signal from insolation changes to the final proxy data employed for time-series analysis.

In our discussion of the pathway of the orbital signal we distinguish between *primary* and *secondary* climate proxies. *Primary* climate proxies are those that are directly influenced (exclusively or non-exclusively) by the climate variable of interest (for example, δD_{ice} and temperature). In contrast, *secondary* climate proxies record a depositional system's response to climate forcing (for example, clay flux via stream discharge into a seaway, responding to precipitation changes). Any given proxy likely represents a composite of multiple *primary* and/or *secondary* climate forcings.

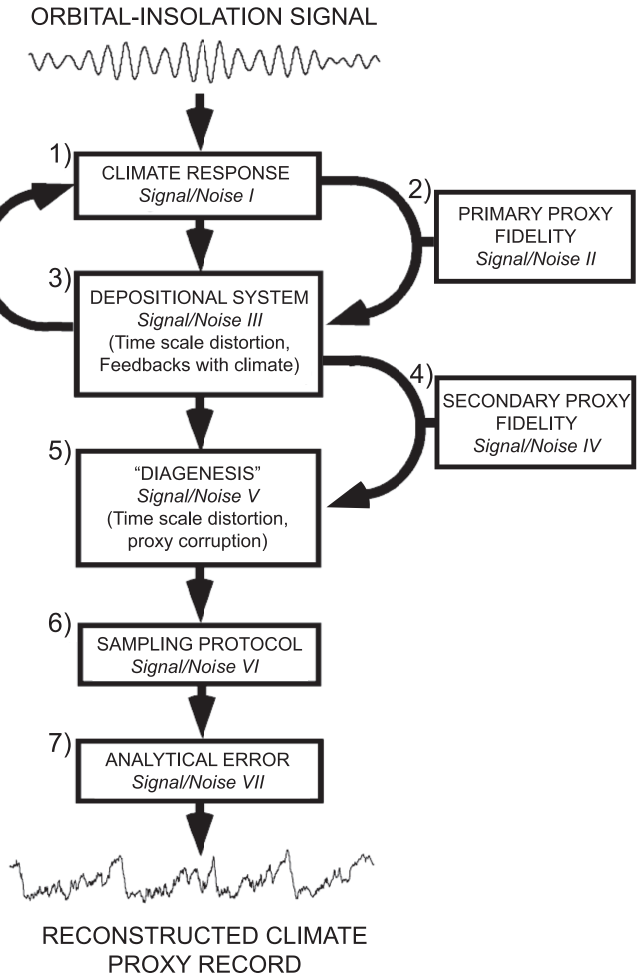

Fig. 1. Theoretical pathway of the orbital signal, from primary insolation changes to the final proxy data series employed for time-series analysis. These steps include 1) the primary response of the climate system to Milankovitch-forced insolation changes, 2) the fidelity of the *primary* climate proxy, 3) the response of the depositional system to the climate forcing, 4) the fidelity of the *secondary* climate proxy, 5) diagenetic alteration of the proxy record, 6) sampling of the paleoclimate record and 7) the analytical error associated with measurement of the proxy signal.

Each step in the path from orbital-insolation signal to proxy (fig. 1) is characterized by a distinctive transfer function that modifies the original insolation signal, and outputs a (orbital) signal to (background) noise ratio. These steps include: 1) the principal response of the climate system to Milankovitch-forced insolation variability, 2) the fidelity of the *primary* proxy response to climate change, 3) the response of the depositional environment to climate, which can distort the relationship between depth and time (for example, changes in the rate of snow accumulation), and potentially involves feedbacks with the climate system (for example, the albedo-temperature feedback and glacier dynamics; Clark and others, 1999), 4) the fidelity of the *secondary* proxy in recording climate-induced depositional system response, 5) diagenetic alteration of the proxy signal, which distorts the relationship between depth and time (compaction) and corrupts the proxy (for example, isotopic exchange, remineralization, *et cetera*), 6) sampling of a paleoclimate record, and 7) the analytical error associated with proxy measurement. The transfer function associated with any one of these steps can potentially diminish an orbital signal. Alternatively, a given transfer function could serve to amplify the orbital signal, or portions of its frequency content (for example, Ripepe and Fisher, 1991; Clark and others, 1999; Rial, 2004a, 2004b). Although not an actual "step" in the pathway of the orbital signal, an additional consideration is the suitability of the statistical methodology used to evaluate the proxy record, and its inherent limitations.

The paramount challenge to accurate assessment of Milankovitch orbital signals in paleoclimate data stems from the fact that the measured climate proxy data series is several steps removed from the climate system response that we seek to quantify ("Signal/Noise I" in fig. 1). Of these steps, the most well-constrained transfer functions are those associated with analytical error ("Signal/Noise VII") and sampling protocol ("Signal/Noise VI"). To guard against the introduction of substantial bias associated with these transfer functions, analytical error must be small relative to the signal variability, while the duration of the record and sample frequency must be great enough to resolve the orbital signal and avoid aliasing. Characterization and deconvolution of the transfer functions associated with steps I-V (fig. 1) are far more difficult, and generally require the implementation of theoretical modeling and advanced signal processing methods (for example, Goreau, 1980; Ripepe and Fisher, 1991; Meyers and others, 2001; Vimeux and others, 2002).

SIGNAL ANALYSIS METHODS

The development and implementation of new signal processing methodologies for quantifying time series has spawned a renaissance in the field of paleoclimatology. In particular, Thomson's (1982) multi-taper method (MTM) for estimation of spectra, and subsequent refinements to the technique (Thomson, 1990; Mann and Lees, 1996) provide a statistically robust platform for assessment of ancient climate variability. In this regard, an important advancement of the MTM technique over previous methods is its treatment of "mixed spectra." Mixed spectra contain one or more periodic components (commonly referred to as phase-coherent sinusoids, harmonics, or lines) imbedded in a background "continuum." The background continuum itself can be further divided into quasiperiodic variability (signals that show a concentration of power in a narrow frequency band, but are not truly phase-coherent) and broadband stochastic noise (for example, "red noise").

Importantly, the MTM technique permits deconvolution of mixed spectra. That is, periodic signals, quasiperiodic signals and the broadband stochastic noise can be distinguished from one another and separately quantified (note that periodic and quasiperiodic signals are collectively referred to as "narrowband" variability in this paper). An important advancement of the technique is its ability to explicitly quantify the power attributable to periodic components (via "harmonic analysis"), which is then removed from the power spectrum to provide a more resilient estimate of the background continuum (termed a "reshaped spectrum"; Thomson, 1982). In addition to this treatment of periodic signals, deconvolution of quasiperiodic signals from broadband noise, which together comprise the continuum, is achieved via autoregressive red noise modeling (Mann and Lees, 1996).

Figure 2 demonstrates the method, using a 400,000 year-long synthetic climate proxy record (fig. 2D). This model is constructed from a 40 kyr periodic signal (fig. 2B), a quasiperiodic signal (whose instantaneous period increases from 60 kyr to 120 kyr through the analysis interval; fig. 2C), and lag-one autoregressive red noise (fig. 2A). The MTM analysis correctly identifies the power attributable to the periodic 40 kyr cycle (gray shaded area in fig. 2E), which is clearly distinguished from the background continuum (the bold black line). Figure 2E also displays confidence level

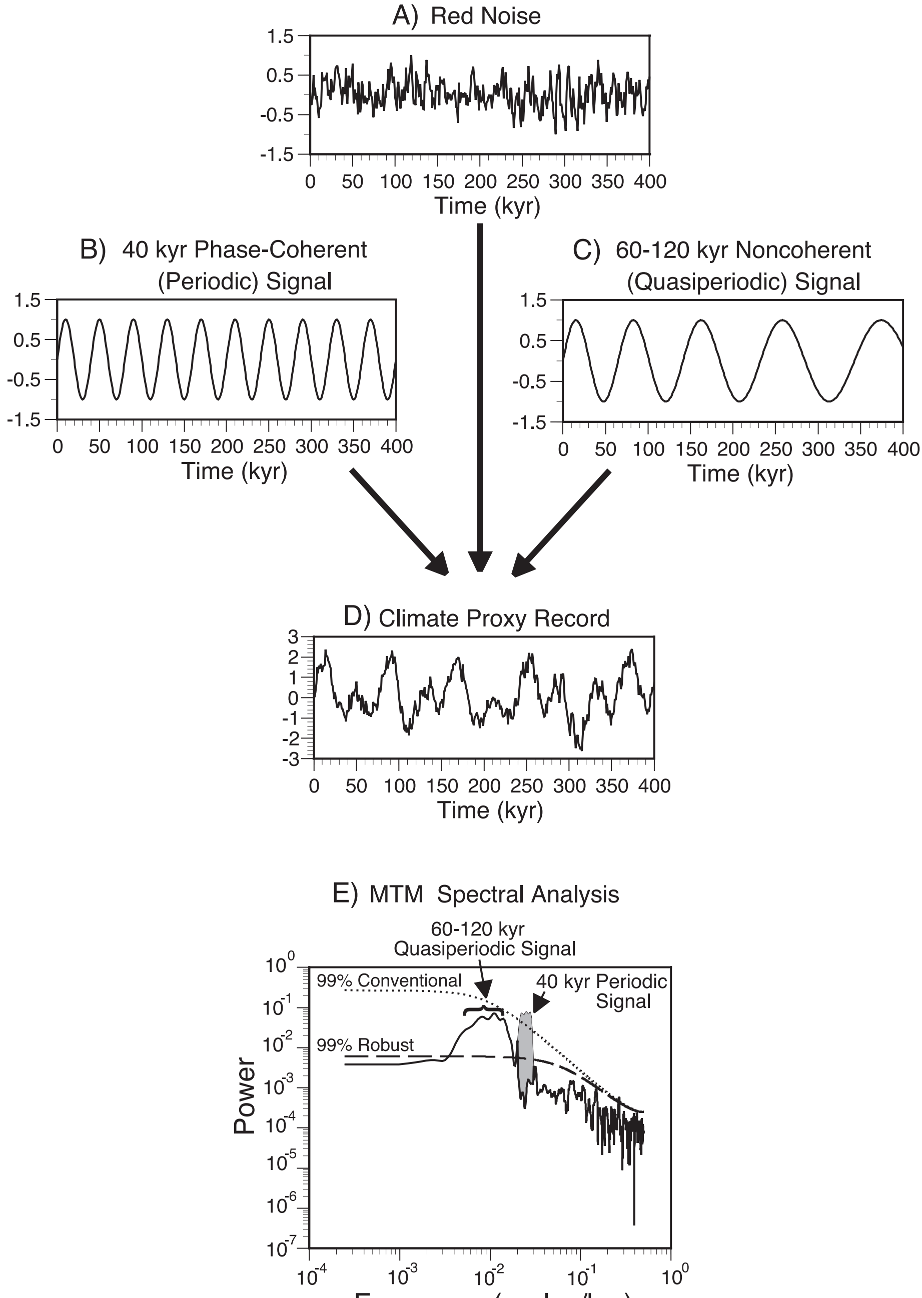

Fig. 2. Deconvolution of periodic signals, quasiperiodic signals, and the broadband noise via application of the multi-taper method. The composite proxy model (D), is composed of a 40 kyr periodic signal (B), a 60–120 kyr quasiperiodic signal (C), and lag-1 autoregressive red noise (A). Part E displays the multi-taper method power spectrum for the composite proxy model, calculated using three 2π data tapers. The method correctly identifies the 40 kyr periodic signal (power attributable to this component is shown in gray), the background continuum (the bold black line), and the 60–120 kyr quasiperiodic signal. The 99% confidence level for the robust red noise model is shown as a dashed line, and the 99% confidence level for the conventional AR(1) red noise model is shown as a dotted line. Note that the robust red noise algorithm used in this study does not utilize spectrum reshaping [in contrast to Mann and Lees (1996)].

estimates for two broadband noise models. We use a conventional autoregressive model (AR(1); Bartlett, 1966), and the robust red noise model of Mann and Lees (1996). The analysis in figure 2E illustrates a crucial point: when strong narrowband signals are present in a time series, they can severely distort the broadband noise estimate provided by conventional autoregressive red noise models. In such cases, it is more appropriate to apply a robust red noise estimate, which fits a lag-one autoregressive model to a median smoothed power spectrum (Mann and Lees, 1996). The robust red noise model correctly identifies the 60 to 120 kyr quasiperiodic signal, and shows superior agreement with the known broadband stochastic noise contribution. Finally, the variance attributable to each of the signals (periodic, quasiperiodic, and broadband noise) can be determined by integration of the power spectrum across the particular frequency bands of interest, and comparison of the "raw" and reshaped spectra.

In practice, the MTM statistical test for periodic signals allows for a weak non-stationarity. Thus, narrowband signals such as the Milankovitch quasiperiods are identified as periodic terms (Thomson, 1990). The concentration of statistically significant power in the orbital bands, and the presence of statistically significant lines at the expected Milankovitch frequencies is strong evidence of orbital influence. We apply this method, as well as a number of additional techniques in our quantitative evaluation of the impact of orbital-insolation changes on climate during the late Pleistocene.

THE VOSTOK TEMPERATURE RECORD

The Antarctica local temperature proxy record of Vimuex and others (2002) is based on $\delta^{18}O_{ice}$ and δD_{ice} measurements from the Vostok ice core. These isotopic records are influenced by a number of factors, including local temperature, the temperature of the moisture source, and changes in ocean isotopic composition (Vimeux and others, 2002). The fidelity of this temperature record ("Signal/Noise II") was maximized by employing a single-trajectory Rayleigh-type isotopic model (Vimeux and others, 2002), which uses δD_{ice} and deuterium excess ($d=\delta D_{ice} - 8\ \delta^{18}O_{ice}$) records from the Vostok ice core in tandem with a stacked record of planktic foraminifera $\delta^{18}O$ values from the Indian Ocean (MD900963 core) and the Pacific Ocean (ODP Site 677) to deconvolve the multiple variables influencing the Vostok isotope record (Bassinot and others, 1994).

Various methodologies attempt to maximize the signal/noise associated with depositional ("Signal/Noise III") and "diagenetic" ("Signal/Noise V") timescale distortion of the Vostok record. These include modeling efforts and orbital tuning techniques that have resulted in a variety of different timescales for the Vostok ice core record (Lorius and others, 1985; Jouzel and others, 1987; Sowers and others, 1993; Jouzel and others, 1993; Waelbroeck and others, 1995; Jouzel and others, 1996; Petit and others, 1999; Shackleton, 2000; Parrenin and others, 2001; Ruddiman and Raymo, 2003). The timescale used by Vimeux and others (2002), Wunsch (2004), and this study is based on the glaciological timescale (GT4) of Petit and others (1999). The GT4 timescale uses a coupled model for glacier dynamics and snow accumulation to remove time-depth distortions from the Vostok proxy record, and also includes two orbitally tuned age control-points (at 110 kyr and 390 kyr). Vimeux and others (2002) further adjusted the timescale for the stacked foraminiferal $\delta^{18}O$ record (Bassinot and others, 1994) to the GT4 timescale (Petit and others, 1999) prior to constructing their temperature proxy series.

Although the Vostok core was originally sampled at a relatively consistent spatial interval (1 m; fig. 3A), the subsequent depth-time transformation necessarily results in an uneven temporal sample spacing of 17 to 664 years ("Signal/Noise VI"; figs. 3B and 3C). Furthermore, each deuterium excess datum from the last climate cycle actually

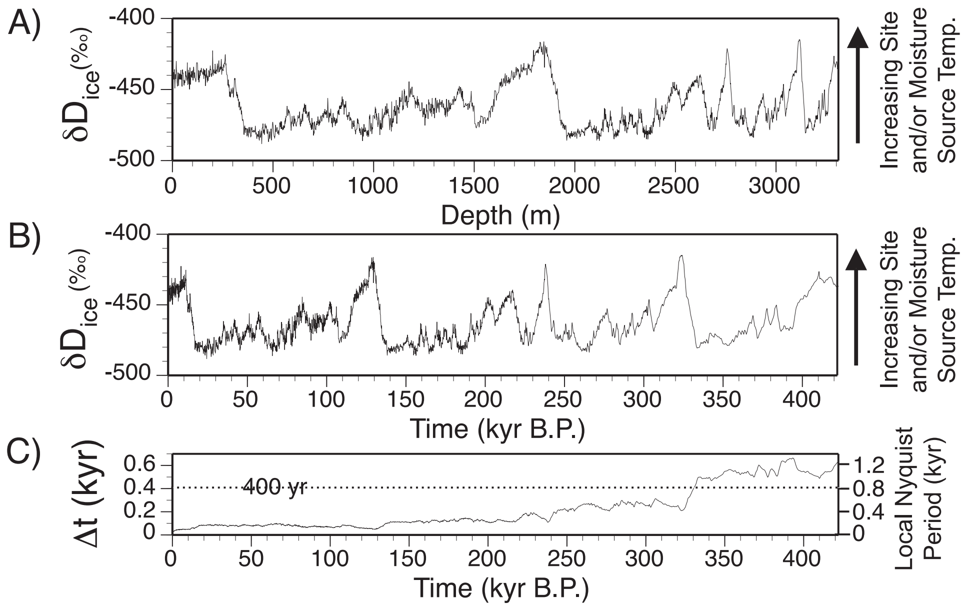

Fig. 3. (A) Vostok deuterium record vs. depth. (B) Vostok deuterium record vs. time, (C) Temporal sampling of the Vostok deuterium record, and associated local Nyquist period.

represents the average of five one-meter samples (F. Vimeux, personal communication), reducing the resolution of the most recent data. Although the data series can be interpolated to an even temporal increment (400 years; Vimeux and others, 2002), the subsequent signal analysis is fundamentally limited by the original sampling. Thus, the highest frequency that can be robustly assessed throughout this isotopic record is ~1/1,328 years (=1/(2*664 years)).

The accuracy of the revised local temperature proxy record of Vimuex and others (2002) is also dependent upon the sampling resolution of the stacked $\delta^{18}O$ time series of Bassinot and others (1994), which was used to reconstruct changes in the ocean isotopic composition. Although the individual data series used to create the $\delta^{18}O$ stack were collected at relatively high resolution (typically <3,000 year sampling interval; Shackleton and others, 1990; Bassinot and others, 1994), the $\delta^{18}O$ data was subsequently smoothed using a moving average procedure (Bassinot and others, 1994; F. Bassinot, personal communication). Due to this smoothing, the most reliable quantification of Vostok temperature variance is limited to periods greater than ~10,000 years. Finally, the analytical errors ("Signal/Noise VII") associated with the Vostok δD measurements (+/- 0.5 per mil), the foraminiferal $\delta^{18}O$ measurements (+/-0.05 per mil), and deuterium excess calculations (+/- 0.7 to 1.3 permil) are small relative to the total variability observed within these records (in all cases less than 15%; Vimeux and others, 2001).

Based on the above discussion of potential distortions in the orbital signal pathway (THE PATHWAY OF THE ORBITAL SIGNAL section), it is clear that a number of uncertainties must be addressed in order to provide an accurate quantification of orbital influence on climate. These include potential inaccuracies in the timescale and additional modifications of the orbital signal via the insolation-climate-depositional system transfer functions (fig. 1). Such factors can be partially addressed with advanced signal analysis methods.

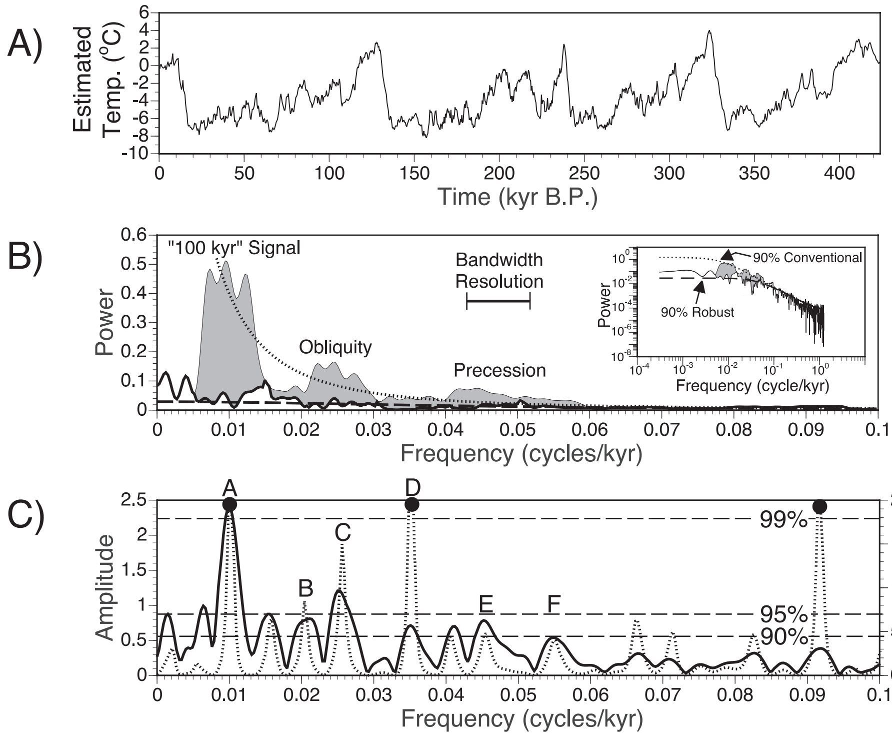

Fig. 4. (A) Vostok site temperature proxy record. Temperatures are expressed as deviations from present-day. (B) MTM power spectrum of the Vostok site temperature proxy record calculated using three 2π data tapers. Also displayed are the 90% confidence level for the conventional red noise model (dotted line), 90% robust red noise confidence level (dashed line), and the reshaped power spectrum (background continuum; bold black line). The conventional red noise confidence level was determined using an AR(1) model, and the robust red noise confidence level was determined using an AR(1) fit to a log-transformed median-smoothed version of the "raw" spectrum (using a 0.25 cycles/kyr smoothing window; see Mann and Lees, 1996). Power attributable to the significant "100 kyr", obliquity-band and precession-band line components (shown in gray) has been removed from the "raw" power spectrum to generate the reshaped spectrum (see equation 500 in Percival and Walden, 1993), yielding an estimate of the background continuum in Vostok temperature over the past 423.6 kyr. Note that the reshaped spectrum is most accurately described by the independently derived robust red noise model. Inset displays a log-log plot of the power spectrum to the Nyquist frequency of 1.25 cycles/kyr, along with red noise confidence levels. (C) MTM harmonic (line) spectrum of the Vostok site temperature proxy record calculated using three 2π data tapers, displaying amplitude (bold line) and F-test results (dotted line). 90%, 95% and 99% significance levels for the F-test results are also shown (dashed lines). F-values have been evaluated using 2 and 4 degrees of freedom. Solid circles identify harmonic components that exceed an F-value of 20. Letters A–F refer to peaks identified in table 1.

QUANTIFICATION OF ORBITAL SIGNALS IN THE VOSTOK TEMPERATURE RECORD

In figure 4, MTM power spectral and harmonic analyses are calculated over the full frequency range of the interpolated (400-year sampling interval) temperature proxy record. Figure 4 also displays confidence level estimates for two noise models, used to determine the significance of the power spectrum results. As indicated in the SIGNAL ANALYSIS METHODS section, the conventional AR(1) noise model can be severely biased if strong narrowband signals are present (see fig. 2E; Mann and Lees, 1996), or when data is interpolated (Schulz and Mudelsee, 2002). In fact, there are a number of strong periodic components in the Vostok data that substantially bias the conventional AR(1) model, as discussed further below.

Table 1

Harmonic components identified in the Vostok site temperature record of Vimuex and others (2002), compared to those observed in the theoretical eccentricity, obliquity and precession signals (Laskar, 1990)

Peak I.D.	Vostok Harmonic Components (kyr/cycle)	Harmonic Probability	Predicted Orbital Components	Percentage Error	Recalibrated Vostok Harmonic Components (kyr/cycle)	Percentage Error
A	99.30	99.68%	109.23 (E)	-9.09%	102.97	-5.74%
B	48.91	96.38%	52.85 (O1)	-7.46%	50.72	-4.04%
C	39.01	98.68%	40.45 (O2)	-3.56%	40.45	0.00%
D	28.49	99.70%	29.00 (O3)	-1.76%	29.54	1.87%
E	21.99	91.25%	23.08 (P1)	-4.72%	22.80	-1.21%
F	18.20	89.01%	18.94 (P2)	-3.91%	18.87	-0.36%

The MTM harmonic analyses were conducted using three 2π data tapers. The recalibrated frequencies have been multiplied by a factor of 1.037 to provide a first order correction of the GT4 timescale error.

The MTM power spectrum indicates three regions of significant power (exceeding the 90% red noise and 90% robust red noise confidence level), corresponding to the eccentricity, obliquity and precession bands (fig. 4B). MTM harmonic analysis of the proxy record detects six significant periodic components within these bands (fig. 4C, table 1). Although additional climatic variance is present in the high-frequency portion of the spectrum (> 1/10,000 years), it likely suffers from poor deconvolution of the multiple controls on the Vostok isotopic signal. In the following analysis we will provide separate estimates that exclude or include this high frequency portion of the spectrum. It is also important to reiterate that assessment of power at frequencies between 1/800 years and 1/1,328 years will be compromised in the oldest portion of the record (330,000−423,600 years) due to decreased temporal resolution of the Vostok ice core (fig. 3C).

To address resolution limitations imposed by sampling protocol ("Signal/Noise VI"), harmonic analysis results for the theoretical orbital parameters (Laskar, 1990) calculated with a 400-year sampling resolution over the past 423,600 years are listed in table 1. Our results indicate that the significant Vostok line components consistently underestimate the expected periodicities (by ~2−9%), which suggests an error in the GT4 timescale. The dominant obliquity term (40,450 years) is known to be the most stable of these orbital periods (Berger and others, 1998), and thus provides an optimal tuning target. Adjustment of the dominant obliquity signal identified in the Vostok record (39,010 years; peak C in fig. 4C) to its predicted value results in reduction of the error associated with 5 of the 6 identified harmonic components, further confirming the timescale error. Note that the time series has not been "re-tuned", but rather the significant frequencies have been multiplied by a factor of 1.037 (40,450 years/39,010 years) to account for the discrepancy between the predicted and observed obliquity values.

To refine our assessment of time-depth distortions in the proxy record, evolutive harmonic analysis (EHA: Park and Herbert, 1987; Yiou and others, 1991; Meyers and others, 2001) is applied (fig. 5). This method permits detection of temporal changes in the amplitude and frequency of the statistically significant harmonic components. Three persistent harmonic components (designated as E, O2, P1) are identified, all of which show a consistent drift to lower frequencies in the upper portion of the proxy record (0-240 kyr). The uniformity of the frequency drift of these three components further confirms distortion of the timescale, which results in smearing of the orbital signal in the power spectrum (fig. 5B) (for example, the 22.80 kyr P1 signal also

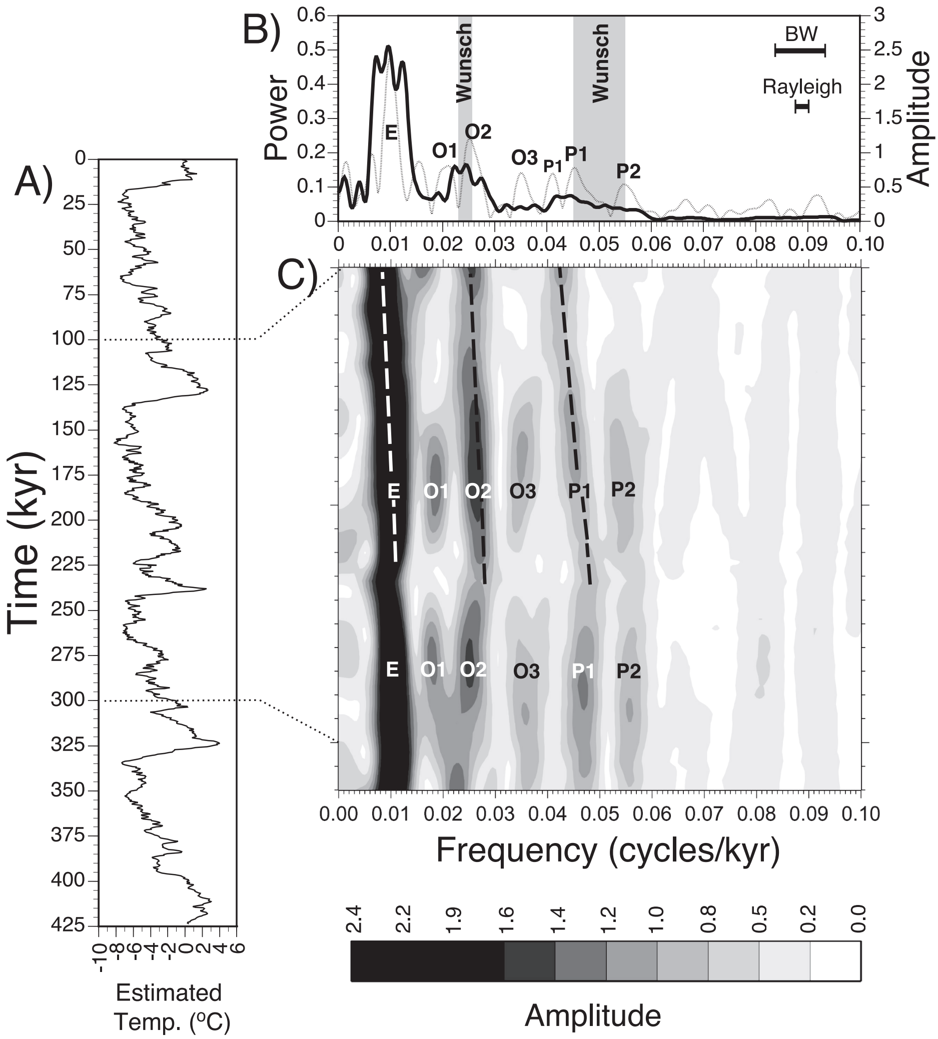

Fig. 5. (A) Vostok site temperature proxy record. (B) MTM power (black bold line) and amplitude (thin dotted line) spectrum for the Vostok site temperature proxy record, calculated using three 2π data tapers. BW=Bandwidth resolution, Rayliegh=Rayleigh resolution. (C) Evolutive harmonic analysis results for the Vostok site temperature proxy record, calculated using three 2π data tapers. The evolutive harmonic analysis employed a 200,000 year moving window and a 4,000 year time step. Note the consistent drift of E, O2 and P1 to lower frequencies in the upper portion of the record, and the intermittent appearance of O1, O3 and P2. The gray area in 5B indicates the portion of the spectrum integrated by Wunsch (2004).

accounts for a significant harmonic component at 24.64 kyr). In addition, this analysis elucidates why the precession periods are characterized by lower significance levels than the eccentricity and obliquity band signals (table 1): these high frequency terms are most severely impacted by the GT4 timescale error.

Guided by the EHA results in figure 5, the fraction of variance attributable to each of the Milankovitch bands can be determined via integration of the power spectrum. Given the timescale errors outlined above, and the bandwidth resolution of the MTM analysis (the fact that the power associated with a given orbital harmonic will be smeared across adjacent frequencies; Thomson, 1982), the area of the spectrum that

Table 2

MTM spectral estimates of the variance attributable to the "1/100,000 year" line component, precession-related lines, obliquity-related lines, and the background continuum in the Vostok temperature proxy series (Vimeux and others, 2002)

	Background Continuum	"100,000" year signal	Obliquity	Precession	Obliquity + Precession
Variance > 800 years	31%	41%	18%	10%	28%
Variance > 10,000 years	28%	43%	19%	10%	29%
Variance in 10-100 kyr band	27%	---	27%	14%	41%
Variance in 10-64 kyr band	34%	---	43%	23%	66%

Note that only seven Milankovitch-band line components have been removed for determination of the background continuum (all other significant lines contribute to the background continuum, thus it is a highly conservative maximum estimate). In calculating these results, the observed frequencies were multiplied by a factor of 1.037 (table 1) to provide a first order correction of the GT4 timescale error. The results show close agreement with those based on the uncorrected GT4 timescale (in all cases $\leq 1\%$).

must be considered in our analysis is quite large. Therefore, it is critical to apply the MTM harmonic analysis to quantify the variance attributable to each periodic component and separate it from the background continuum ("spectral reshaping"; Thomson, 1982; Percival and Walden, 1993). These factors were not considered in the estimate provided by Wunsch (2004) (see gray area in fig. 5B).

Comparison of the Vostok temperature power spectrum with the reshaped spectrum (fig. 4B; table 2) indicates that 41 percent of the variance at periods > 800 years is attributable to a strongly periodic "100,000" year cycle, 28 percent is attributable to the precession and obliquity periods, and 31 percent is attributable to a background continuum that resembles the robust red noise model of Mann and Lees (1996). The fact that the robust red noise model provides superior agreement with the independently estimated "reshaped spectrum" confirms its applicability to the Vostok temperature proxy record. If we restrict our analysis to frequencies $< 1/10{,}000$ years, the most reliable region of the spectrum for assessment of Antarctica temperature, the variance attributable to the precession and obliquity components increases to 29 percent, and the "100,000" year cycle accounts for 43 percent of the variance. Additional analyses accounting for other frequency bands of interest establish that the precession and obliquity periods account for 41 percent of the variance in the 1/10 kyr – 1/100 kyr band, and 66 percent of the variance in the 1/10kyr – 1/64 kyr band (the latter of which avoids all of the power attributable to the "100,000" year cycle). Our results are substantially greater that those previously published by Wunsch (2004), and thus establish the importance of precession and obliquity band signals in so-called "myriennial"-scale climate change (*sensu* Wunsch, 2004; 1/10 kyr-1/100 kyr).

Influence of the glacial/interglacial "saw-tooth"

A striking feature of the Vostok temperature proxy record is the "saw-tooth" shape of the glacial/interglacial cycles. Non-sinusoidal characteristics have important consequences for Fourier-based spectral analysis methods, which reconstruct the observed signal using idealized sinusoids of varying frequency, amplitude and phase. The most important artifact of the "saw-tooth" pattern in recent climate records is the generation of multiple overtones in the spectrum, some of which may coincidentally contribute power within the precession and obliquity frequency bands.

To address this issue, we model the glacial/interglacial saw-tooth signal using a linear-least squares fitting procedure. Data that span each peak interglacial to peak glacial are individually fit to a linear model, and these linear segments are then assembled into a composite record (fig. 6A). Spectral analysis of the resultant saw-

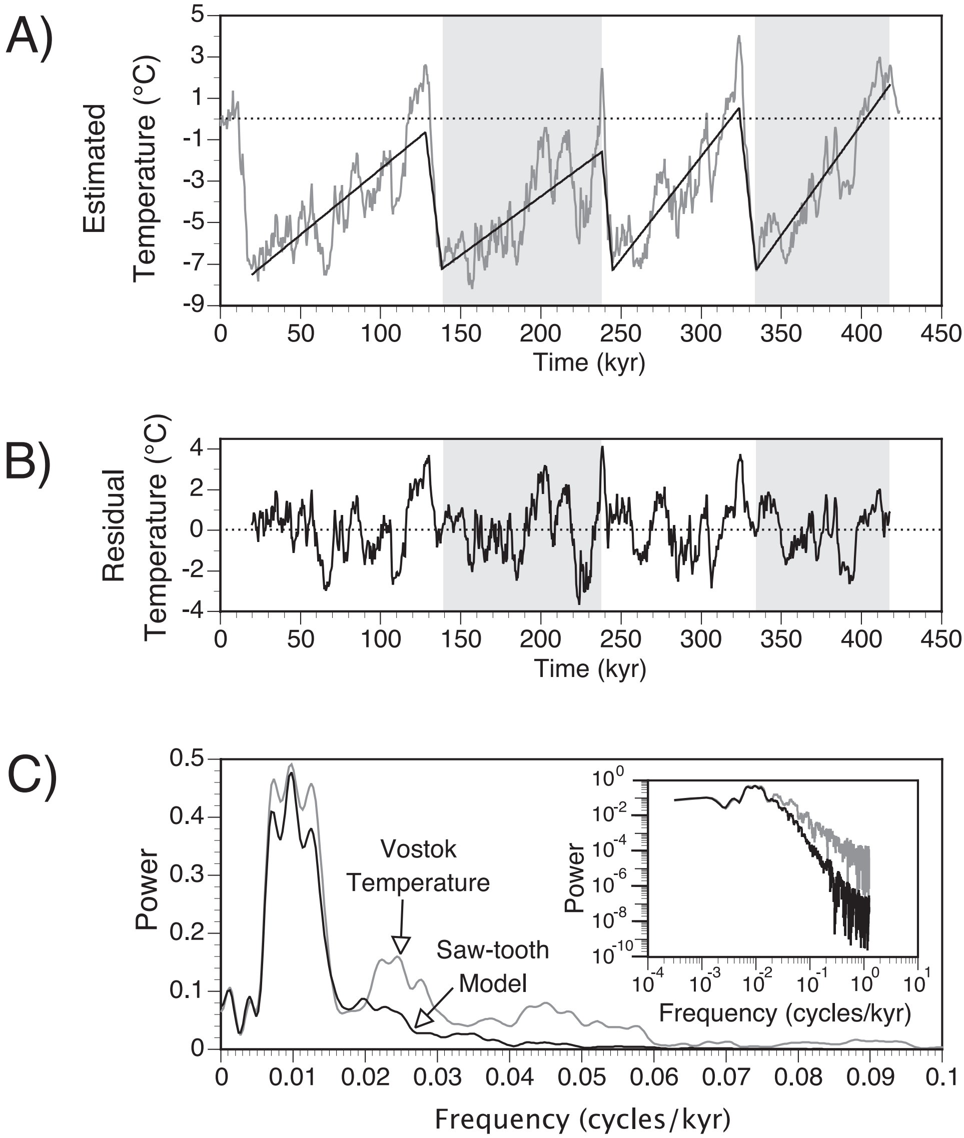

Fig. 6. (A) Vostok site temperature proxy record (gray line) and saw-tooth model (black line). (B) Residual temperature not accounted for by the saw-tooth model shown in figure 6A. (C) MTM power spectral estimates for the saw-tooth model (black line) and the Vostok site temperature proxy record (gray line), calculated using three 2π data tapers. Both spectral analyses utilize time series that extend from 19.6 kyr to 418.0 kyr. Inset displays a log-log plot of the power spectra to the Nyquist frequency of 1.25 cycles/kyr.

tooth model allows estimation of its contribution to power in the precession and obliquity bands (fig. 6C).

MTM spectral analysis of the saw-tooth model captures 87 percent of the variance associated with the Vostok temperature proxy ~100,000 year cycle. In addition, up to 54 percent of the obliquity signal variance could be an artifact of the saw-tooth shape, as well as up to 14 percent of the precession signal variance. However, these estimates include a contribution from the background continuum. Based on our analysis, the saw-tooth shape of the glacial/interglacial cycles has a substantial impact on the Vostok obliquity band variance, but much less of an impact on precession band variance. If we attribute all of saw-tooth derived variance to the periodic components measured in the QUANTIFICATION OF ORBITAL SIGNALS IN THE VOSTOK TEMPERATURE RECORD section (an overly optimistic assumption), then 17 percent of the variance < 1/800 years is attributable to precession and obliquity forcing, as well as 17 percent of the variance < 1/10000 years, 25 percent of the variance between 1/10-1/100 kyr, and 39 percent of the variance between 1/10 to 1/64 kyr.

DISCUSSION

Our analysis indicates that Vostok temperature variance is almost equally apportioned between three components: direct "forcing" from the precession and obliquity orbital-insolation changes (28%), a periodic "100,000" year cycle (41%), and the background continuum (31%). A range of analyses accounting for various frequency bands of interest, and potential bias introduced by the "saw-tooth" shape of the glacial/interglacial cycle, establish that precession and obliquity periods account for between 25 to 41 percent of the variance in the 1/10 kyr to 1/100 kyr band, and between 39 to 66 percent of the variance in the 1/10kyr to 1/64 kyr band. These results are two to four times greater than recent estimates of the same Vostok time series. In all cases, most of the remaining variance is accounted for by the "100,000" year cycle, which is distinct from a background continuum that resembles autoregressive red noise.

The predominance of 1/100,000 year variance in the spectrum, with a strong periodic character (fig. 4C), and high coherence with orbital eccentricity (for example, see Shackleton, 2000), suggests a dominant link to orbital changes. A number of studies have suggested that the 100,000 year cycle may be "paced" by precession and/or obliquity driven orbital-insolation changes (in contrast to direct "forcing" by eccentricity; Hays and others, 1976; Raymo, 1997; Ridgwell and others, 1999; Huybers and Wunsch, 2005; Tziperman and others, 2006). For example, Huybers and Wunsch (2005) demonstrate a link between obliquity variability and the timing of glacial terminations. However, due to timescale uncertainties it is not yet possible to provide a definitive test for a precession-scale driver of glacial terminations (Huybers and Wunsch, 2005). Given the inherent modulation of precession by eccentricity, such a linkage could plausibly explain the observed "100,000" cycle, and its strong coherence to the theoretical eccentricity signal (Shackleton, 2000).

As for the physical mechanism(s) responsible for this "100,000" cycle, a wide range of hypotheses have been proposed (for example, Liu, 1992; Imbrie and others, 1993; Berger and others, 1999; Clark and others, 1999; Ruddiman, 2003; Rial, 2004a; and many others). For example, Ruddiman (2003) suggested that several spatially dependent insolation-climate transfer functions (affecting green house gas concentrations) can interact to generate the 100,000 year cycle. Alternatively, the 100,000 year signal could be the consequence of an interplay between orbitally forced climate variations and glacier dynamics. In this regard, changes in the character of the underlying geological substrate can play a key role in generating the 100,000 year cycle, and/or the interaction of positive (ice-albedo) and negative (moisture availability) glacier feedbacks (for example, Clark and others, 1999; Rial, 2004a).

Regardless of the precise mechanism, a strong statistical relationship between the orbital signal and this 100,000 year cycle (for example, Rial, 1999; Shackleton, 2000; Huybers and Wunsch, 2005) confirms that, at a minimum, the cycle is entrained by the orbital signal. While Milankovitch's (1947) original insolation-climate hypothesis did not predict strong eccentricity power, *a priori* dismissal of the 100-kyr power as non-orbital (forced or paced) assumes that all of the transfer functions (fig. 1) are purely linear, which clearly need not be the case (see Imbrie and others, 1993; Roe and

Allen, 1999; Hinnov, 2000; Elkibbi and Rial, 2001; Rial, 2004a, 2004b; Rial and others, 2004). Given the fact that non-linear phenomena are a common aspect of the Earth System (for example, the thermodynamic phase transition from vapor to liquid water, *et cetera*) we should anticipate that non-linear mechanisms at least partially characterize the climate and climate recorder (depositional system) transfer functions and/or the response of *primary* or *secondary* climate proxies, and that such responses can potentially link the 100 kyr power to an orbital-insolation signal.

CONCLUSIONS

In this study we have outlined the factors that complicate accurate assessment of orbital forcing in paleoclimate proxy records and have employed a template to provide a quantitative estimate of the impact of orbital-insolation changes on climate during the late Pleistocene. Our analysis indicates that Vostok temperature variance is almost equally apportioned between direct "forcing" from the precession and obliquity orbital-insolation changes (28%), a periodic "100,000" year cycle (41%), and the background continuum (31%). These results substantially deviate from the analysis of Wunsch (2004), which concluded that the Vostok record is dominated by stochastic noise, with no more than 7 percent of the signal attributable to orbital changes. Differences in these estimates reflect fundamentally different conclusions regarding the controls on climate over orbital time scales and the fidelity of geological records of climate forcing.

Importantly, our analysis considers the following criteria that have not been addressed previously:

1. *Resolution limitations associated with core sampling (Signal/Noise VI) and power spectral analysis.* Due to the smoothing inherent in spectral estimation, power attributable to periodic variability will be distributed across a broader finite bandwidth. For example, given a 2π MTM spectrum of the Vostok record (which was used in this study and represents a relatively high-resolution estimate), recovery of variance attributable to a 40,000-year signal requires integration of the power spectrum across the bandwidth 1/33,651 years to 1/49,302 years. Such bandwidth smoothing was not considered by Wunsch (2004).
2. *Use of a robust model of background noise (Mann and Lees, 1996).* This is necessary because the conventional red noise modeling technique, based on a first order autoregressive process, is biased if strong periodic components are embedded in the paleoclimate signal (Mann and Lees, 1996), as is the case in the Vostok temperature record.
3. *Consideration of the insolation-climate-depositional system transfer functions (Signal/Noise I and III) and proxy response (Signal/Noise II and IV), which potentially amplify weak insolation signals and distort the orbital signal.* Detection of the orbital periods was conducted via application of the MTM harmonic analysis approach, to quantify statistically significant periodic components (phase-coherent sinusoids) in the time series. By specifically testing for the orbital line frequencies, and comparing the measured values with the theoretical values, we identified an error in the GT4 timescale. Evolutive Harmonic Analysis was used to further characterize this timescale distortion. The analysis of Wunsch (2004) did not apply the MTM harmonic analysis approach to test for the orbital line components, nor time-frequency analysis methods to assess potential timescale problems. Integration of the spectrum across the narrow bands employed by Wunsch (2004) (40–45 kyr; 18–22 kyr) misses fractions of the power due to O2, P1 and P2, and neglects the power attributable to O1 and O3 (see fig. 5B).
4. *Application of an MTM "reshaping" algorithm (Thomson, 1982; Percival and Walden,*

1993) to estimate the background continuum. Application of this method was possible because we explicitly tested for the presence of periodic components using MTM harmonic analysis. Importantly, the reshaped spectrum is consistent with the robust red noise model, which is independently derived. Finally, comparison of the original and reshaped power spectrum permits an estimate of the climate variance attributable to the orbital periods.

5. *Consideration of the spectral artifacts associated with the saw-tooth shape of the "100,000" year cycle.* These spectral artifacts were found to constitute a substantial fraction of the variance in the Vostok obliquity band signal.

The largest source of error in our analysis is attributable to proxy fidelity (Signal/Noise II and IV). Although an attempt has been made to deconvolve the multiple controls on the Vostok isotopic record (Vimuex and others, 2002), a number of uncertainties remain, such as the impact of initial atmospheric isotopic composition and variable hydrologic conditions during vapor transport (Vimeux and others, 2002). Nevertheless, given the current status of the Vostok site temperature proxy, Milankovitch orbital control (forcing and/or pacing) accounts for the majority of the ~12°C temperature variability observed in Antarctica over the past 423,600 years, and thus supports orbital variability and associated changes in insolation as a fundamental control on global climate change during the Pleistocene.

ACKNOWLEDGMENTS

This study was partially funded by the Yale Institute for Biospheric Studies Gaylord Donnelley Environmental Fellowship (SRM). We acknowledge Francoise Vimeux, Franck Bassinot, Jose Rial, and Linda Hinnov for insightful discussions. We also thank Francoise Vimeux for providing the Vostok site temperature proxy record and the adjusted Bassinot and others (1994) data. Thoughtful comments by two anonymous reviewers substantially improved this manuscript.

REFERENCES

Bartlett, M. S., 1966, An Introduction to Stochastic Processes: Cambridge, United Kingdom, Cambridge University Press, 362 p.

Bassinot, F. C., Labeyrie, L. D., Vincent, E., Quidelleur, X., Shackleton, N. J., and Lancelot, Y., 1994, The astronomical theory of climate and the age of the Brunhes-Matuyama magnetic reversal: Earth and Planetary Science Letters, v. 126, p. 91–108, doi:10.1016/0012-821X(94)90244-5.

Berger, A., Loutre, M. F., and Melice, J. L., 1998, Instability of the astronomical periods from 1.5 Myr BP to 0.5 Myr AP: Paleoclimates, v. 2, p. 239–280.

Berger, A., Li, X. S., and Loutre, M. F., 1999, Modelling Northern Hemisphere ice volume over the last 3 Ma: Quaternary Science Reviews, v. 18, p. 1–11, doi:10.1016/S0277-3791(98)00033-X.

Clark, P. U., Alley, R. B., and Pollard, D., 1999, Northern hemisphere ice-sheet influences on global climate change: Science, v. 286, p. 1104–1111, doi:10.1126/science.286.5442.1104.

Elkibbi, M., and Rial, J. A., 2001, An outsider's review of the astronomical theory of the climate: is the eccentricity-driven insolation the main driver of the ice ages?: Earth-Science Reviews, v. 56, p. 161–177, doi:10.1016/S0012-8252(01)00061-7.

Goreau, T. J., 1980, Frequency sensitivity of the deep-sea climatic record: Nature, v. 287, p. 620–622, doi:10.1038/287620a0.

Hays, J. D., Imbrie, J., and Shackleton, N. J., 1976, Variations in the Earth's orbit: Pacemaker of the ice ages: Science, v. 194, p. 1121–1132, doi:10.1126/science.194.4270.1121.

Herbert, T. D., 1994, Reading orbital signals distorted by sedimentation: models and examples, *in* de Boer, P. L., and Smith, D. G., editors, Orbital Forcing and Cyclic Sequences: Oxford, Blackwell Scientific Publications, International Association of Sedimentologists, Special Publication 19, p. 483–507.

Herbert, T. D., and Fischer, A. G., 1986, Milankovitch climatic origin of mid-Cretaceous black shale rhythms in central Italy: Nature, v. 321, p. 739–743, doi:10.1038/321739a0.

Hinnov, L. A., 2000, New perspectives on orbitally forced stratigraphy: Annual Reviews of Earth and Planetary Science, v. 28, p. 419–475, doi:10.1146/annurev.earth.28.1.419.

Huybers, P., and Wunsch, C., 2005, Obliquity pacing of the late Pleistocene glacial terminations: Nature, v. 434, p. 491–494, doi:10.1038/nature03401.

Imbrie, J., Berger, A., Boyle, E. A., Clemens, S. C., Duffy, A., Howard, W. R., Kukla, G., Kutzbach, J., Martinson, D. G., McIntyre, A., Mix, A. C., Molfino, B., Morley, J. J., Peterson, L. C., Pisias, N. G., Prell, W. L., Raymo, M. E., Shackleton, N. J., and Toggweiler, J. R., 1993, On the structure and origin of major glaciation cycles: 2. The 100,000-year cycle: Paleoceanography, v. 8, p. 699–735.

Jouzel, J., Lorius, C., Petit, J. R., Genthon, C., Barkov, N. I., Kotlyakov, V. M., and Petrov, V. M., 1987, Vostok ice core: a continuous isotope temperature record over the last climatic cycle (160,000 years): Nature, v. 329, p. 403–408, doi:10.1038/329403a0.

Jouzel, J., Barkov, N. I., Barnola, J. M., Bender, M., Chappelaz, J., Genthon, C., Kotlyakov, V. M., Lipenkov, V., Lorius, C., Petit, J. R., Raynaud, D., Raisbeck, G., Ritz, C., Sowers, T., Stievenard, M., Yiou, F., and Yiou, P., 1993, Extending the Vostok ice-core record of paleoclimate to the penultimate glacial period: Nature, v. 364, p. 407–412, doi:10.1038/364407a0.

Jouzel, J., Waelbroeck, C., Malaiz, B., Bender, M., Petit, J. R., Stievenard, M., Barkov, N. I., Barnola, J. M., King, T., Kotlyakov, V. M., Lipenkov, V., Lorius, C., Raynaud, D., Ritz, C., and Sowers, T., 1996, Climatic interpretation of the recently extended Vostok ice records: Climate Dynamics, v. 12, p. 513–521, doi:10.1007/BF00207935.

Kominz, M. A., and Pisias, N. G., 1979, Pleistocene climate: Deterministic or stochastic?: Science, v. 204, p. 171–173, doi:10.1126/science.204.4389.171.

Laskar, J., 1990, The chaotic motion of the solar system: A numerical estimate of the chaotic zones: Icarus, v. 88, p. 266–291, doi:10.1016/0019-1035(90)90084-M.

Laurin, J., Meyers, S. R., Sageman, B. B., and Waltham, D., 2005, Phase-lagged amplitude modulation of hemipelagic cycles: A potential tool for recognition and analysis of sea-level change: Geology, v. 33, p. 569–572, doi:10.1130/G21350.1.

Liu, H. S., 1992, Frequency variations of the Earth's obliquity and the 100-kyr ice-age cycles: Nature, v. 358, p. 397–399, doi:10.1038/358397a0.

Lorius, C., Jouzel, J., Ritz, C., Merlivat, L., Barkov, N. I., Korotkevitchand, Y. S., and Kotlyakov, V. M., 1985, A 150,000-year climatic record from Antarctic ice: Nature, v. 316, p. 591–596, doi:10.1038/316591a0.

Mann, M. E., and Lees, J. M., 1996, Robust estimation of background noise and signal detection in climatic time series: Climate Change, v. 33, p. 409–445, doi:10.1007/BF00142586.

Meyers, S., Sageman, B., and Hinnov, L., 2001, Integrated Quantitative Stratigraphy Of The Cenomanian-Turonian Bridge Creek Limestone Member Using Evolutive Harmonic Analysis And Stratigraphic Modeling: Journal of Sedimentary Research, v. 71, p. 628–644, doi:10.1306/012401710628.

Milankovitch, M., 1941, Kanon der Erdbestrahlung und seine Andwendung auf das Eiszeitenproblem: Belgrade, Königlich Serbische Akademie (Royal Serbian Academy), 633 p.

Olsen, P. E., 1986, A 40-Million-Year Lake Record of Early Mesozoic Orbital Climatic Forcing: Science, v. 234, p. 842–848, doi:10.1126/science.234.4778.842.

Park, J., and Herbert, T. D., 1987, Hunting for paleoclimatic periodicities in a geologic time series with an uncertain time scale: Journal of Geophysical Research, v. 92, B13, p. 14,027–14,040, doi:10.1029/JB092iB13p14027.

Parrenin, F., Jouzel, J., Waelbroeck, C., Ritz, C., and Barnola, J. M., 2001, Dating Vostok ice core by an inverse method: Journal of Geophysical Research, v. 106(D23), p. 31837–31851.

Pelletier, J. D., 2002, Natural variability of atmospheric temperatures and geomagnetic intensity over a wide range of time scales: PNAS (Proceedings of the National Academy of Sciences), v. 99, Supplement 1, p. 2546–2553, doi:10.1073/pnas.022582599.

Percival, D. B., and Walden, A. T., 1993, Spectral Analysis for Physical Applications: Multitaper and Conventional Univariate Techniques: Cambridge, Cambridge University Press, 583 p.

Pestiaux, P., and Berger, A., 1984, Impacts of deep-sea processes on paleoclimate spectra, *in* Berger, A., Imbrie, J., Hays, G., Kukla, G., and Saltzman, B., editors, Milankovitch and Climate, Part 1: Dordrecht, Reidel Publishing, Part 1, p. 493–510.

Petit, J. R., Jouzel, J., Raynaud, D., Barkov, N. I., Barnola, J. M., Basile, I., Bender, M., Chappellaz, J., Davis, M., Delaygue, G., Delmotte, M., Kotlyakov, V. M., Legrand, M., Lipenkov, V. Y., Lorium, C., Pepin, L., Ritz, C., Saltzman, E., and Stievenard, M., 1999, Climate and atmospheric history of the past 420,000 years from the Vostok ice core, Antarctica: Nature, v. 399, p. 429–436, doi:10.1038/20859.

Raymo, M. E., 1997, The Timing of Major Climate Terminations: Paleoceanography, v. 12, p. 577–585, doi:10.1029/97PA01169.

Rial, J. A., 1999, Pacemaking the Ice Ages by Frequency Modulation of Earth's Orbital Eccentricity: Science, v. 285, p. 564–568, doi:10.1126/science.285.5427.564.

——— 2004a, Abrupt climate change: chaos and order at orbital and millennial scales: Global and Planetary Change, v. 41, p. 95–109, doi:10.1016/j.gloplacha.2003.10.004.

——— 2004b, Earth's orbital eccentricity and the rhythm of the Pleistocene ice ages: the concealed pacemaker: Global and Planetary Change, v. 41, p. 81–93, doi:10.1016/j.gloplacha.2003.10.003.

Rial, J. A., Pielke, R. A., Sr., Beniston, M., Claussen, M., Canadell, J., Cox, P., Held, H., Noblet-Ducoudre, N., Prinn, R., Reynolds, J. F., and Salas, J. D., 2004, Nonlinearities, feedbacks and critical thresholds within the Earth's climate system: Climatic Change, v. 65, p. 11–38, doi:10.1023/B:CLIM.0000037493.89489.3f.

Ridgwell, A. J., Watson, A. J., and Raymo, M. E., 1999, Is the spectral signature of the 100 kyr glacial cycle consistent with a Milankovtich origin?: Paleoceanography, v. 14, p. 437–440, doi:10.1029/1999PA900018.

Ripepe, M., and Fischer, A. G., 1991, Stratigraphic rhythms synthesized from orbital variations, *in* Franseen, E. K., Watney, W. L., Kendall, D.G.St.C., and Ross, W., editors, Sedimentary Modeling; Computer Simulations and Methods for Improved Parameter Definition: Kansas State Geological Survey Bulletin 233, p. 335–344.

Roe, G. H., and Allen, M. R., 1999, A comparison of competing explanations for the 100,000-yr ice age cycle: Geophysical Research Letters, v. 26, p. 2259–2262, doi:10.1029/1999GL900509.

Ruddiman, W. F., 2003, Orbital insolation, ice volume, and greenhouse gases: Quaternary Science Reviews, v. 22, p. 1597–1629, doi:10.1016/S0277-3791(03)00087-8.

Ruddiman, W. F., and Raymo, M. E., 2003, A methane-based time scale for Vostok ice: Quaternary Science Reviews, v. 22, p. 141–155, doi:10.1016/S0277-3791(02)00082-3.

Sageman, B. B., Rich, J., Arthur, M. A., Birchfield, G. E., and Dean, W. E., 1997, Evidence For Milankovitch

periodicities in Cenomanian-Turonian lithologic and geochemical cycles, Western Interior U.S.A.: Journal of Sedimentary Research, v. 67, p. 286–302.
Saltzman, B., 1982, Stochastically-driven climatic fluctuations in the sea-ice, ocean temperature, CO_2 feedback system: Tellus, v. 34, p. 97–112.
Schulz, M., and Mudelsee, M., 2002, REDFIT: estimating red-noise spectra directly from unevenly spaced paleoclimatic time series: Computers and Geosciences, v. 28, p. 421–426, doi:10.1016/S0098-3004(01)00044-9.
Shackleton, N. J., 2000, The 100,000-year ice age cycle identified and found to lag temperature, carbon dioxide, and orbital eccentricity: Science, v. 289, p. 1897–1902, doi:10.1126/science.289.5486.1897.
Shackleton, N. J., Berger, A., and Peltier, W. R., 1990, An alternative astronomical calibration of the lower Pleistocene timescale based on ODP Site 677: Transactions of the Royal Society of Edinburgh, Earth Sciences, v. 81, p. 251–261.
Sowers, T., Bender, M., Labeyrie, L. D., Jouzel, J., Raynaud, D., Martinson, D., and Korotkevich, Y. S., 1993, A 135,000 year Vostok - SPECMAP common temporal framework: Paleoceanography, v. 8, p. 737–766, doi:10.1029/93PA02328.
Thomson, D. J., 1982, Spectrum estimation and harmonic analysis: IEEE Proceedings, v. 70, p. 1055–1096, doi:10.1109/PROC.1982.12433.
——— 1990, Quadratic-Inverse Spectrum Estimates: Applications to Palaeoclimatology: Philosophical Transactions of the Royal Society of London A, v. 332, p. 539–597, doi:10.1098/rsta.1990.0130.
Tziperman, E., Raymo, M. E., Huybers, P., and Wunsch, C., 2006, Consequences of pacing the Pleistocene 100 kyr ice ages by nonlinear phase locking to Milankovitch forcing: Paleoceanography, v. 21, PA4206, doi:10.1029/2005PA001241, doi:10.1029/2005PA001241.
Vimeux, F., Masson, V., Delaygue, G., Jouzel, J., Petit, J. R., and Stievenard, M., 2001, A 420,000 year deuterium excess record from East Antarctica: Information on past changes in the origin of precipitation at Vostok: Journal of Geophysical Research, v. 106, D23, p. 31,863–31,873, doi:10.1029/2001JD900076.
Vimeux, F., Cuffey, K. M., and Jouzel, J., 2002, New insights into Southern Hemisphere temperature changes from Vostok ice cores using deuterium excess correction: Earth and Planetary Science Letters, v. 203, p. 829–843, doi:10.1016/S0012-821X(02)00950-0.
Waelbroeck, C., Jouzel, J., Labeyrie, L., Lorius, C., Labracherie, M., Stiévenard, M., and Barkov, N. I., 1995, A Comparison of the Vostok ice deuterium record and series from Southern Ocean core MD 88-770 over the last two glacial-interglacial cycles: Climate Dynamics, v. 12, p. 113–123, doi:10.1007/BF00223724.
Weedon, G. P., and Jenkyns, H. C., 1999, Cyclostratigraphy and the Early Jurassic timescale: Data from the Belemnite Marls, Dorset, southern England: The Geological Society of America Bulletin, v. 111, p. 1823–1840, doi:10.1130/0016-7606(1999)111⟨1823:CATEJT⟩2.3.CO;2.
Wunsch, C., 2003, The spectral description of climate change including the 100 ky energy: Climate Dynamics, v. 20, p. 353–363, doi 10.1007/s00382-002-0279-z.
——— 2004, Quantitative estimate of the Milankovitch-forced contribution to observed Quaternary climate change: Quaternary Science Reviews, v. 23, p. 1001–1012, doi:10.1016/j.quascirev.2004.02.014.
Yiou, P., Genthon, C., Ghil, M., Jouzel, J., Le Treut, H., Barnola, J., Lorius, C., and Korotkevitch, Y., 1991, High-Frequency paleovariability in climate and CO_2 levels from Vostok ice core records: Journal of Geophysical Research, v. 96, B12, p. 20,365–20,378, doi:10.1029/91JB00422.
Zachos, J., Pagani, M., Sloan, L., Thomas, E., and Billups, K., 2001, Trends, rhythms, and aberrations in global climate 65 Ma to present: Science, v. 292, p. 686–693, doi:10.1126/science.1059412.